JOURNAL OF VIROLOGY, Dec. 2002, p. 12008–12022 Vol. 76, No. 23
0022-538X/02/$04.00+0 DOI: 10.1128/JVI.76.23.12008–12022.2002

Distinct Poly(rC) Binding Protein KH Domain Determinants for Poliovirus Translation Initiation and Viral RNA Replication

Brandon L. Walter,[1] Todd B. Parsley,[1]† Ellie Ehrenfeld,[2] and Bert L. Semler[1]*

Department of Microbiology and Molecular Genetics, College of Medicine, University of California, Irvine, California 92697,[1] and Laboratory of Infectious Diseases, National Institute of Allergy and Infectious Diseases, National Institutes of Health, Bethesda, Maryland 20892[2]

Received 6 June 2002/Accepted 27 August 2002

The limited coding capacity of picornavirus genomic RNAs necessitates utilization of host cell factors in the completion of an infectious cycle. One host protein that plays a role in both translation initiation and viral RNA synthesis is poly(rC) binding protein 2 (PCBP2). For picornavirus RNAs containing type I internal ribosome entry site (IRES) elements, PCBP2 binds the major stem-loop structure (stem-loop IV) in the IRES and is essential for translation initiation. Additionally, the binding of PCBP2 to the 5′-terminal stem-loop structure (stem-loop I or cloverleaf) in concert with viral protein 3CD is required for initiation of RNA synthesis directed by poliovirus replication complexes. PCBP1, a highly homologous isoform of PCBP2, binds to poliovirus stem-loop I with an affinity similar to that of PCBP2; however, PCBP1 has reduced affinity for stem-loop IV. Using a dicistronic poliovirus RNA, we were able to functionally uncouple translation and RNA replication in PCBP-depleted extracts. Our results demonstrate that PCBP1 rescues RNA replication but is not able to rescue translation initiation. We have also generated mutated versions of PCBP2 containing site-directed lesions in each of the three RNA-binding domains. Specific defects in RNA binding to either stem-loop I and/or stem-loop IV suggest that these domains may have differential functions in translation and RNA replication. These predictions were confirmed in functional assays that allow separation of RNA replication activities from translation. Our data have implications for differential picornavirus template utilization during viral translation and RNA replication and suggest that specific PCBP2 domains may have distinct roles in these activities.

Following entry into a host cell, the single-stranded, positive-sense genomic RNA of poliovirus (PV) must provide a nucleation point for the formation of numerous ribonucleoprotein (RNP) complexes. These complexes are capable of mediating the three major processes that the RNA must undergo to establish a successful infection of the host cell. The PV genomic RNA must be translated, replicated, and packaged for a productive virus infection to ensue. Given the small size (~7,400 nucleotides [nt]) of the PV genome, the virus has evolved to utilize numerous proteins or other molecular machinery resident in the host cell to carry out its infectious cycle. One example of the molecular scavenging necessitated by the limited coding capacity of PV is utilization of a single cellular RNA-binding protein, poly(rC) binding protein 2 (PCBP2), for the formation of RNP complexes that form on two different PV 5′ noncoding region (5′ NCR) RNA secondary structures to mediate two of the three above-mentioned processes (16, 24, 25, 50).

PCBP2 (also known as hnRNP E2 and αCP-2) is a cellular RNA-binding protein that interacts with the 5′ NCR of PV RNA (14, 15, 23). The protein contains three hnRNP K-homology (KH) RNA-binding domains and has a binding preference for poly(rC). In in vitro binding studies, the first and third KH domains appear to mediate the poly(rC)-binding activity (22). PCBP2 mRNA is widely expressed, and the protein has been detected in both the cytoplasm and the nucleus of human cells (36). PCBP2 has been shown to form homodimers and has been found to interact with other hnRNP proteins, including hnRNP I (also known as polypyrimidine tract-binding protein or PTB), hnRNP K, and hnRNP L (24, 34). Many of the above characteristics are shared by a highly homologous (83% identical at the nucleic acid level and 90% similar at the amino acid level) isoform, PCBP1. This protein (also known as hnRNP E1 and αCP-1) is hypothesized to have been generated by retrotransposition of a fully processed PCBP2 mRNA into the mammalian genome prior to the mammalian radiation (39). PCBP1 was first described as a poly(C)-binding protein that was widely expressed in diverse tissue types (1). While PCBP1 and PCBP2 are the major PCBP isoforms expressed in mammalian cells, transcripts of two additional PCBP isoforms, PCBP3 and PCBP4, have been detected at low levels in human and mouse tissues (40).

To date, PCBP1 and PCBP2 are known to be components of two types of functional RNP complexes that form on cellular mRNAs. While both types of RNP complexes form on RNA elements found in the 3′ NCRs of mRNAs, one type of complex regulates stability and the other type regulates translation of these mRNAs. The association of PCBP with the 3′ NCRs of the α-globin (19, 33, 59–61), β-globin (63), α(I)-collagen (38, 54), and the tyrosine hydroxylase (51) mRNAs are four known examples of PCBP associating in functional RNP complexes on cellular mRNAs to impart stability to these mRNAs

* Corresponding author. Mailing address: Department of Microbiology and Molecular Genetics, College of Medicine, University of California, Irvine, CA 92697-4025. Phone: (949) 824-7573. Fax: (949) 824-8598. E-mail: blsemler@uci.edu.

† Present address: University of Maryland Biotechnology Institute, Center for Agricultural Biotechnology, College Park, MD 20742-4450.

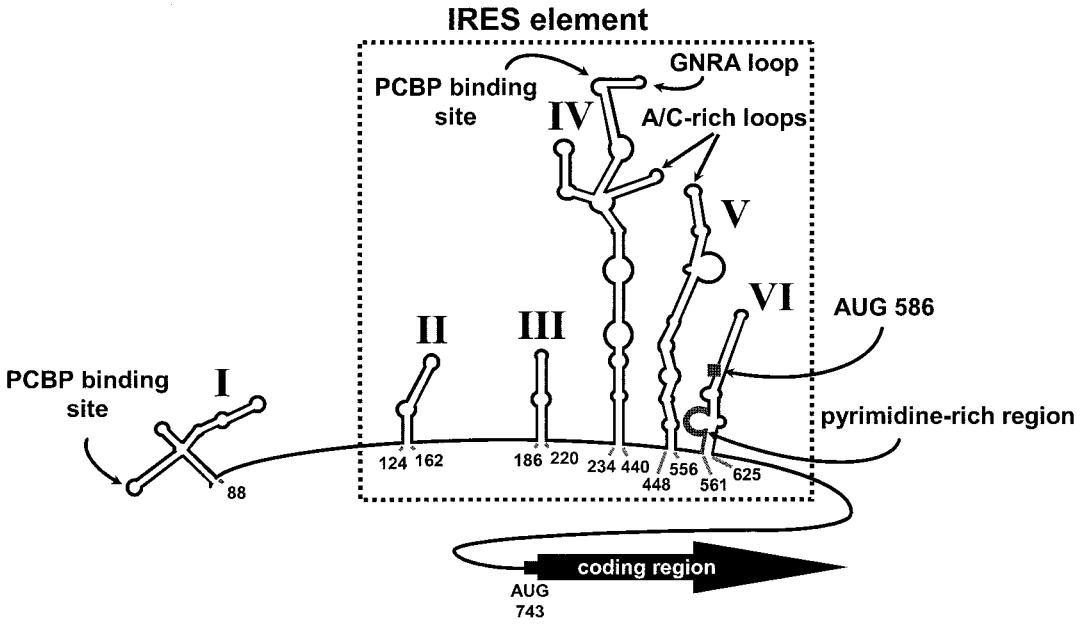

FIG. 1. Predicted RNA secondary structure of the PV 5′ NCR. The RNA conformation is based upon computer prediction that is supported by chemical and enzymatic structure probing data. The six major stem-loop structures, including the 5′-terminal cloverleaf (stem-loop I) and the major stem-loop of the PV IRES element (stem-loop IV), are indicated in roman numerals. The minimal IRES element is boxed by a dashed line. 5′ NCR elements that are highly conserved across the *Picornaviridae*, including a GNRA tetraloop, A/C-rich loops, and a pyrimidine-rich domain, are shown. Putative PCBP binding sites on stem-loop I and stem-loop IV RNA, as determined by genetic, biochemical, and functional data, are designated (15, 16, 24, 26, 50). A conserved upstream AUG codon (nt 586) is also indicated. Nucleotide numbers are indicated below the structure. (Adapted from reference 55 with the permission of Elsevier Science.)

(32). A similar RNP complex has also been found to form on the 3′ NCR of erythropoietin mRNAs (21). The formation of an RNP complex (containing hnRNP K and PCBP1) on a CU-rich repetitive sequence motif found in the 3′ NCR of the 15-lipoxygenase mRNA is an example of the second type of complex that appears to regulate translation by inhibition of the 60S ribosomal subunit joining the 40S subunit at the initiating AUG codon (48, 49).

Beyond the role of PCBP in cellular mRNA stability and translational control, a number of functions relating to viral gene expression have been ascribed to the protein. For PV, the interactions of PCBP with specific RNA secondary structural domains contained within the 5′ NCR of the genomic RNA are involved in translation, replication, and possibly stability of the RNA. Baltimore and colleagues first implicated the formation of an RNP complex (that contained the PV protein, 3CD, and an unidentified ~36-kDa cellular protein) on PV stem-loop I (refer to Fig. 1) as important for PV RNA synthesis (4, 5). The ~36-kDa cellular protein that was present in this functionally significant complex was later shown to be PCBP2 (50). This finding was confirmed and expanded to include the related protein PCBP1 (24). Interestingly, in addition to the role of PCBP in replication of PV RNA, a mechanism evolved to utilize this cellular protein in cap-independent translation initiation on the PV internal ribosome entry site (IRES) element. This mechanism is mediated by an RNP complex that includes PCBP2 and stem-loop IV of the PV IRES (15, 16, 24). The functional duality of PCBP in its mediation of two separate mechanisms led Andino and Gamarnik to hypothesize that PCBP could function together with viral protein 3CD to regulate these processes (24–26). Additionally, the formation of the stem-loop I/PCBP RNP complex has been implicated as contributing to the stability of PV genomic RNA in a HeLa cell-free PV translation-RNA replication assay (44). Finally, PCBP has been found to function in the life cycle of human papillomavirus type 16 as a regulator of late gene expression (20).

In addition to its well-documented functions in the PV life cycle, PCBP2 also plays a role in the life cycles of other picornaviruses. Based upon sequence and structural similarities shared between certain picornavirus IRES elements, two major IRES classifications have been defined. While enterovirus and rhinovirus IRES elements are classified as type I IRES elements, the cardiovirus and aphthovirus IRES elements comprise a group of type II elements (55, 62). Despite the fact that the 5′ NCRs of all picornaviruses tested interact with PCBP2 in vitro, those 5′ NCRs that contain type II IRES elements (encephalomyocarditis virus [EMCV] and foot-and-mouth disease virus) do not require PCBP for IRES-mediated translation in vitro, while the type I IRES elements of PV, coxsackievirus, and human rhinovirus all utilize PCBP for translation (58). The IRES element of hepatitis A virus cannot be easily classified into either of the major IRES classes; however, PCBP2 plays a role in the translation of hepatitis A virus genomic RNA (27).

Although we have considerable information about the compositions of RNP complexes formed with different regions of picornavirus genomic RNAs, the mechanisms by which such complexes function are not well understood (for a review, see reference 3). The present study investigated the roles of PCBP-

mediated RNP complexes in PV cap-independent translation and RNA replication. Specifically, we analyzed the PCBP domains required for the formation of two distinct RNP complexes, one that binds PV stem-loop I in concert with 3CD and another that associates with PV stem-loop IV, which are required for genomic RNA replication and translation, respectively. Because the replication of picornavirus genomic RNA requires viral proteins that are generated during translation of the RNA, replication is dependent upon translation. This functional duality of PCBP makes it impossible to examine the effects of PCBP depletion on PV RNA replication without affecting translation. Therefore, we utilized a chimeric, dicistronic PV replicon (based upon pT7-PV1-E2A [42]) to uncouple translation from RNA replication by use of the EMCV IRES element to drive translation of the PV proteins that are necessary for RNA replication. We examined in vitro PV IRES-mediated translation and PV RNA replication in extracts depleted of PCBP. Upon add-back of recombinant PCBP, our results demonstrated that PCBP1 is able to rescue PV RNA replication with an efficiency equal to that of PCBP2 but is not able to efficiently rescue translation initiation. Additionally, we have generated mutated versions of PCBP2 containing site-directed lesions in each of the three KH domains. The defects in the ability of these mutated proteins to interact with stem-loop I or stem-loop IV in vitro, coupled with data from functional assays, suggest that the individual KH domains may have differential functions in PV translation and RNA replication.

MATERIALS AND METHODS

Plasmid design. Synthetic oligonucleotides (primers) were as follows: PV3C(+) (5′-ATTGTTACAGCAACTACTAGCA-3′); *Eco*RI-MluI-PolyT(−) (5′-CCCGAATTCACGCGTTTTTTTTTTTTTTTTTTTTTTTTTTTT-3′); mKH1(+) (5′-ATCATCGGAGCGGCAGGAGAATCAGTTAAGGCGATGGCCGAGGAGAGT-3′); mKH1(−) (5′-ACTCTCCTCGGCCATCGCCTTAACTGATTCTCCTGCCGCTCCGATGAT-3′); mKH2(+) (5′-CTCATTGGAGCAGGTGGATGCAAGATCGCGGAAATAGCAGAGAGTACA-3′); mKH2(−) (5′-TGTACTCTCTGCTATTTCCGCGATCTTGCATCCACCTGCTCCAATGAG-3′); mKH3(+) (5′-ATAATCGGGGCTCAAGCGCCAAAATCAATGAGATCGCTCAGATGTCT-3′); mKH3(−) (5′-AGACATCTGAGCGATCTCATTGATTTTGGCGCCTTGAGCCCCGATTAT-3′). Plasmids pT7-5′NCR (28) and pT220-460 (23) have been previously described.

The T7-based transcription plasmid pT7RibPVE2A(MluI) was generated through the production of three subclones, pT7PV1(MluI), pT7PVE2A(2MluI), and pT7PVE2A(MluI). pT7PV1(MluI) was generated by direct cloning of PCR-amplified sequences corresponding to the final ~0.4 kb of the PV genome into the *Pvu*II (PV nt 7055) and *Eco*RI (a unique vector site) sites of pT7PV1 (28). This PCR product was amplified from pT7PV1 utilizing a PV3C(+)/*Eco*RI-MluI-PolyT(−) primer set. The *Acc*I(PV nt 6219)/*Pvu*I(a unique vector site) fragment of pT7PV1 (MluI), the *Pvu*I(a unique vector site)/*Nhe*I(PV nt 2470) fragment of pT7PV1, and the *Nhe*I(PV nt 2470)/*Acc*I(PV nt 6219) fragment of pT7-PV-E2A (kindly provided by A. Paul and E. Wimmer [42]) were gel purified and incubated with T4 DNA ligase to generate pT7PVE2A(2MluI). The pT7PVE2A(2MluI) subclone was digested in two separate reactions with *Acc*I (PV nt 6219) and *Nhe*I(PV nt 2470) in one reaction and *Nhe*I(PV nt 2470) and *Nde*I(PV nt 3672) in the other reaction. These two fragments were gel purified and incubated with T4 DNA ligase in a three-fragment ligation reaction with the gel-purified *Nde*I(PV nt 3672)/*Acc*I(PV nt 6219) fragment of pT7PV1 to form the plasmid pT7PVE2A(MluI). The *Stu*I(a unique vector site)/*Sgr*AI(PV nt 339) fragment of prib(+)RLuc (30), which contains a *cis*-acting hammerhead ribozyme adjacent to the first 339 nt of the PV 5′ NCR, was cloned directly into the *Sgr*AI(PV nt 339) and *Stu*I(a unique vector site) sites of the subclone pT7PVE2A(MluI). The orientation, sequence, and junctions of pT7RibPVE2A (MluI) were confirmed by DNA sequence analysis.

Site-directed mutagenesis of regions encoding putative RNA binding domains within the PCBP2 bacterial expression vector pQE30-PCBP2 (15) were generated using oligonucleotide mismatch mutagenesis (35, 47) with a Stratagene QuickChange site-directed mutagenesis kit. Site-directed mutations coding for amino acid changes K31A, K32A, K38A, and R40A in PCBP2 KH domain 1 were generated using synthetic oligonucleotides mKH1(+) and mKH1(−). Site-directed mutations coding for amino acid changes K115A, K121A and R124A in PCBP2 KH domain 2 were engineered using synthetic oligonucleotides mKH2(+) and mKH2(−). Site-directed mutations coding for amino acid changes R305A and R314A in PCBP2 KH domain 3 were engineered using synthetic oligonucleotides mKH3(+) and mKH3(−). Mutations in all expression plasmids were confirmed by dideoxynucleotide sequencing. Upon sequence analysis, the site-directed mutagenesis scheme resulted in the plasmids pQE30-PCBP2-mKH1-2 (coding for amino acid changes K31A, K32A, K38A, and R40A), pQE30-PCBP2-mKH2-6 (coding for amino acid changes K121A and R124A), pQE30-PCBP2-mKH3-3 (coding for amino acid change R314A), and pQE30-PCBP2-mKH3-4 (coding for amino acid changes R305A and R314A).

Transcription and purification of RNA. RNA probes for use in RNA electrophoretic mobility shift assays were generated by run-off transcription using bacteriophage T7 RNA polymerase as described previously (13). Briefly, pT7-5′NCR linearized with *Dde*I was used as template to generate the radiolabeled stem-loop I RNA probe (corresponding to the first 108 nt of PV). pT220-460 linearized with *Hin*dIII was used as template to generate the radiolabeled stem-loop IV RNA probe containing PV nt 220 to 460 preceded by 9 nt and followed by 6 nt of pGEM-1-derived vector sequences. Both probes were gel purified on an 8% polyacrylamide urea gel, and following overnight elution in elution buffer (0.5 M ammonium acetate, 1 mM EDTA, and 0.1% sodium dodecyl sulfate [SDS]) they were ethanol precipitated, resuspended in diethyl pyrocarbonate-treated water, and quantified based on specific activity.

The RibPVE2A(MluI) dicistronic replicon RNA used to program the in vitro translation-transcription reactions was generated by T7-based run-off transcription on a pT7RibPVE2A(MluI) template that was linearized with *Mlu*I. The RNA was synthesized as described previously (18) with the following exceptions: (i) the reaction volumes were 100 μl, (ii) 50 ng of *Mlu*I-linearized pT7RibPVE2A(MluI) transcription template was used per microliter of reaction mixture, (iii) 1.0 U of placental RNasin (Promega) was used per microliter of reaction mixture, (iv) 2.5 U of T7 RNA polymerase (New England Biolabs) was used per microliter of reaction mixture, and (v) the incubations were carried out at 37°C for 2.5 to 3 h. Following transcription, the RNAs were extracted with phenol-chloroform and ethanol precipitated in the presence of ammonium acetate. The precipitated RNAs were then washed two times with 70% ethanol, resuspended in diethyl pyrocarbonate-treated water, and quantitated by agarose gel electrophoresis and ethidium bromide staining with known quantities of similar-sized RNAs.

Purification of recombinant PCBP (rPCBP). Purification of hexahistidine-tagged PCBP2, mutated PCBP2, and PCBP1 was performed essentially as previously described (50). Briefly, PCBP was purified from isopropyl-β-D-thiogalactopyranoside-induced *Escherichia coli* JM109 cells carrying pQE30-PCBP2 or pQE30-PCBP1 (15) or derivatives of pQE30-PCBP2 containing site-directed mutations including pQE30-PCBP2-mKH1-2, pQE30-PCBP2-mKH2-6, pQE30-PCBP2-mKH3-3, and pQE30-PCBP2-mKH3-4. The conditions for growth, induction of protein expression, and purification of PCBP2 were identical to the previously described methods. Prior to use in RNA mobility shift assays or in vitro translation-replication reactions, the purified proteins were dialyzed overnight at 4°C against 4 liters of initiation factor buffer (5 mM Tris-HCl [pH 7.4], 100 mM KCl, 0.05 mM EDTA, 1 mM dithiothreitol, 5% glycerol [17]). The purity and quantity of PCBP was determined by SDS-polyacrylamide gel electrophoresis (SDS-PAGE) analysis and the Bradford protein assay (Bio-Rad). The protein fractions used in these experiments were determined to be >95% pure by Coomassie blue staining.

RNA electrophoretic mobility shift analysis. RNA mobility shift assays were performed essentially as previously described (5, 13). Briefly, purified rPCBP2, mutated rPCBP2, or rPCBP1 was incubated in the presence of RNA binding buffer (5 mM HEPES-KOH [pH 7.4], 25 mM KCl, 2.5 mM $MgCl_2$, 20 mM dithiothreitol, 3.8% [vol/vol] glycerol, 1 mg of *E. coli* tRNA [Sigma]/ml, 8 U of RNasin [Promega], and 0.5 mg of bovine serum albumin [New England Biolabs]/ml) with radiolabeled PV stem-loop I or stem-loop IV RNA probe. The final concentration of probe was 0.1 nM contained within a total reaction volume of 10 μl. This reaction was incubated for 10 min at 30°C. Following incubation, 2.5 μl of 50% glycerol was added and the resulting complexes were resolved at 4°C on native 4% polyacrylamide gels.

HeLa S10 preparation. Extracts were prepared essentially as previously described (7, 17), with the following modifications: (i) HeLa cells were resuspended in a volume of hypotonic buffer equal to that of the cell pellet, (ii) the cells were lysed by as few strokes of the glass Dounce homogenizer as possible to obtain

95% lysis, as assayed by trypan blue exclusion, (iii) the extract was treated with 120 U of micrococcal S7 nuclease (Worthington Biochemical) per ml of S10 supernatant at 13°C for 15 min, and (iv) EGTA was added to a final concentration of 4 mM for inactivation of the nuclease. The HeLa S10 translation extracts were stored under liquid nitrogen.

HeLa (RSW) preparation. HeLa cell ribosomal salt wash (RSW) was prepared essentially by previously described protocols (7, 17). The only modification was the clarification of the dialyzed RSW by centrifugation for 10 min at 3,000 rpm in a Beckman JA-20 rotor. The RSW preparation was then stored under liquid nitrogen.

RNA affinity chromatography depletion of HeLa cell translation extracts. A poly(rC) RNA affinity column [1 g of poly(C) agarose (Sigma) containing ~2.5 mg of coupled poly(rC)] and a column containing agarose matrix only (agarose-adipic acid hydrazide [Pharmacia]) were washed extensively with binding buffer [20 mM HEPES-KOH (pH 7.4), 1.3 mM Tris-HCl (pH 7.5), 33 mM KCl, 80 mM $K(CH_3CO_2)$, 3.7 mM $Mg(CH_3CO_2)_2$, 4.3 mM dithiothreitol, 13 μM EDTA, 1.3% glycerol] before use. Following the wash, a ~4-ml mixture containing 74% HeLa S10 and 26% HeLa RSW was divided into two equal volumes. One aliquot of the HeLa cell extract was applied to the poly(rC) RNA affinity column, while the other volume was applied to the respective mock column to which no RNA was coupled. Each flowthrough was collected and was reapplied to the column three additional times. Following the fourth pass over the RNA affinity or mock column, the poly(rC)-depleted or mock-depleted HeLa cell translation extracts were stored under liquid nitrogen. The columns were recycled for additional depletions by extensive washes in 2 M KCl followed by Tris-EDTA. All poly(rC)-depleted or mock-depleted extracts were prepared at 4°C.

In vitro translation-RNA replication reactions. The translation-RNA replication reaction mixtures (50 μl) contained 68% (by volume) HeLa S10/RSW [poly(rC)-depleted or mock-depleted], 1.25 μg of RibPVE2A(MluI) RNA, 16 mM HEPES-KOH (pH 7.4), 60 mM $K(CH_3CO_2)$, 1 mM ATP, 250 μM GTP, 250 μM UTP, 30 mM creatine phosphate (Boehringer Mannheim), 400 μg of creatine-kinase (Boehringer Mannheim) per ml, and 16% (by volume) RSW buffer (17) in the absence or presence of rPCBP2, mutated rPCBP2, or rPCBP1. Additionally, negative controls for RNA replication contained 2 mM guanidine hydrochloride. Reaction mixtures were split into two portions, with a 10-μl portion for translation analysis and a 40-μl portion for analysis of RNA replication. The 10-μl portion was supplemented with 15 μCi of [^{35}S]methionine (specific activity, >1,000 Ci/mmol; Amersham Pharmacia Biotech) and guanidine hydrochloride to a final concentration of 2 mM. Both aliquots were incubated at 30°C for 4.5 h. The translation reaction mixtures were diluted in Laemmli sample buffer, boiled, and subjected to SDS-PAGE on a 12.5% gel. The RNA replication reaction mixtures were supplemented with 25 μCi of [α-^{32}P]CTP (specific activity, 3,000 Ci/mmol; Amersham Pharmacia Biotech), and incubation was continued at 34°C for 2.5 h. Total RNA was isolated from these RNA replication reaction mixtures using an RNAqueous Total RNA Isolation kit (Ambion). Recovered RNA was then subjected to gel electrophoresis on a 1.0% agarose TBE (90 mM Tris-borate, 0.1 mM EDTA) gel containing ethidium bromide. In an adjacent lane, ~1 μg of RibPVE2A(MluI) RNA was loaded to visualize the mobility of the single-stranded dicistronic RNA. Images of both the translation and replication gels are based upon scans of phosphor storage screens performed with a Personal Molecular Imager FX (Bio-Rad), and quantitation of these scans was performed with the accompanying software package Quantity One (Bio-Rad).

RESULTS

PCBP1 and PCBP2 have differential capacities to bind PV stem-loops I and IV. To examine the possibility that PCBP1 functions similarly to PCBP2 in both translation and replication of PV RNA, we performed in vitro RNA binding assays to compare the binding activities of both proteins on PV stem-loops I and IV. Previous in vitro RNA binding assays using crude extracts from bacteria expressing rPCBP1 demonstrated that stem-loop IV was unable to form specific RNP complexes with these extracts (15). Subsequently, Gamarnik and Andino (24) reported that PCBP1 could interact with both stem-loop I and stem-loop IV RNA; however, in that report the in vitro RNA binding assays utilized rPCBP at single high doses (i.e. ~2.5 μM). At this high protein concentration in the absence of a dose response, it is difficult to distinguish the affinity of PCBP1 and PCBP2 for stem-loop IV RNA or to correlate complex formation to in vivo function. Therefore, to examine and compare the binding affinities of PCBP1 and PCBP2 for PV stem-loop I and stem-loop IV RNA sequences, we carried out in vitro RNA electrophoretic mobility shift assays using purified rPCBP1 and rPCBP2 proteins and radiolabeled stem-loop I and IV RNA probes (Fig. 2A and B, respectively).

As seen in Fig. 2A, the incubation of increasing molar amounts of either rPCBP2 or rPCBP1 with 0.1 nM stem-loop I RNA resulted in the formation of specific RNP complexes. The affinity of rPCBP2 and rPCBP1 for stem-loop I sequences appeared to be nearly equivalent or perhaps slightly reduced for rPCBP1. This differed from the relative affinities of the two proteins for stem-loop IV RNA sequences (Fig. 2B). While the incubation of 0.1 nM stem-loop IV RNA with as little as 0.5 nM PCBP2 (Fig. 2B, lane 2) resulted in the formation of a specific PCBP2/stem-loop IV RNP complex, disappearance of free stem-loop IV RNA probe was not observed until approximately 500 nM PCBP1 was used (Fig. 2B, lane 11). As concentrations of rPCBP1 were increased, the levels of uncomplexed stem-loop IV RNA probe continued to diminish while different RNP complexes with decreased electrophoretic mobility formed (Fig. 2B, lanes 12 to 14). Although the composition of the different PCBP1/stem-loop IV RNP complexes was unclear, the various complexes could represent PCBP1-PCBP1 multimerization events, the binding of PCBP1 to lower-affinity binding sites within stem-loop IV RNA, or the oligomerization of multiple PCBP1/stem-loop IV complexes.

These in vitro RNA binding studies demonstrated that PCBP2 and PCBP1 have near-equal affinities for stem-loop I RNA sequences, but PCBP2 had a much higher binding affinity for stem-loop IV RNA than did PCBP1. Upon comparison of Fig. 2A, lanes 2 to 9, and Fig. 2B, lanes 2 to 8, these data also suggested that PCBP2 has a higher affinity for stem-loop IV than for stem-loop I under the conditions of these in vitro binding assays.

PCBP2 mediates PV RNA translation and replication, while PCBP1 mediates only replication. To determine whether the data derived from the in vitro binding assays correlate with the ability of PCBP1 and PCBP2 to mediate the formation of functional RNP complexes on PV stem-loops I and IV, we utilized an in vitro PV translation-replication assay (7, 43, 56). In this assay, HeLa cell cytoplasmic (S10) extract supplemented with HeLa RSW was programmed with T7 RNA polymerase-transcribed PV RNA. Endogenous PCBP contained in the HeLa cell cytoplasmic extracts was depleted by passage of the extracts over an affinity column containing matrix coupled to poly(rC) (Fig. 3, compare lanes 1 and 2). While there is variability from extract to extract in the efficiency of PCBP depletion, all extracts utilized in the following studies were depleted of PCBP to levels comparable to those observed in Fig. 3, as determined by Western blot analysis. For comparison, we included a sample of purified rPCBP2 that contains a hexahistidine tag at the amino terminus, thereby accounting for the electrophoretic mobility differences seen in the figure. Since both translation and replication of PV RNA are impaired upon PCBP depletion (16, 24, 50), the involvement of PCBP1 in these processes could be determined by addition of rPCBP1, leading to the rescue of in vitro translation and/or

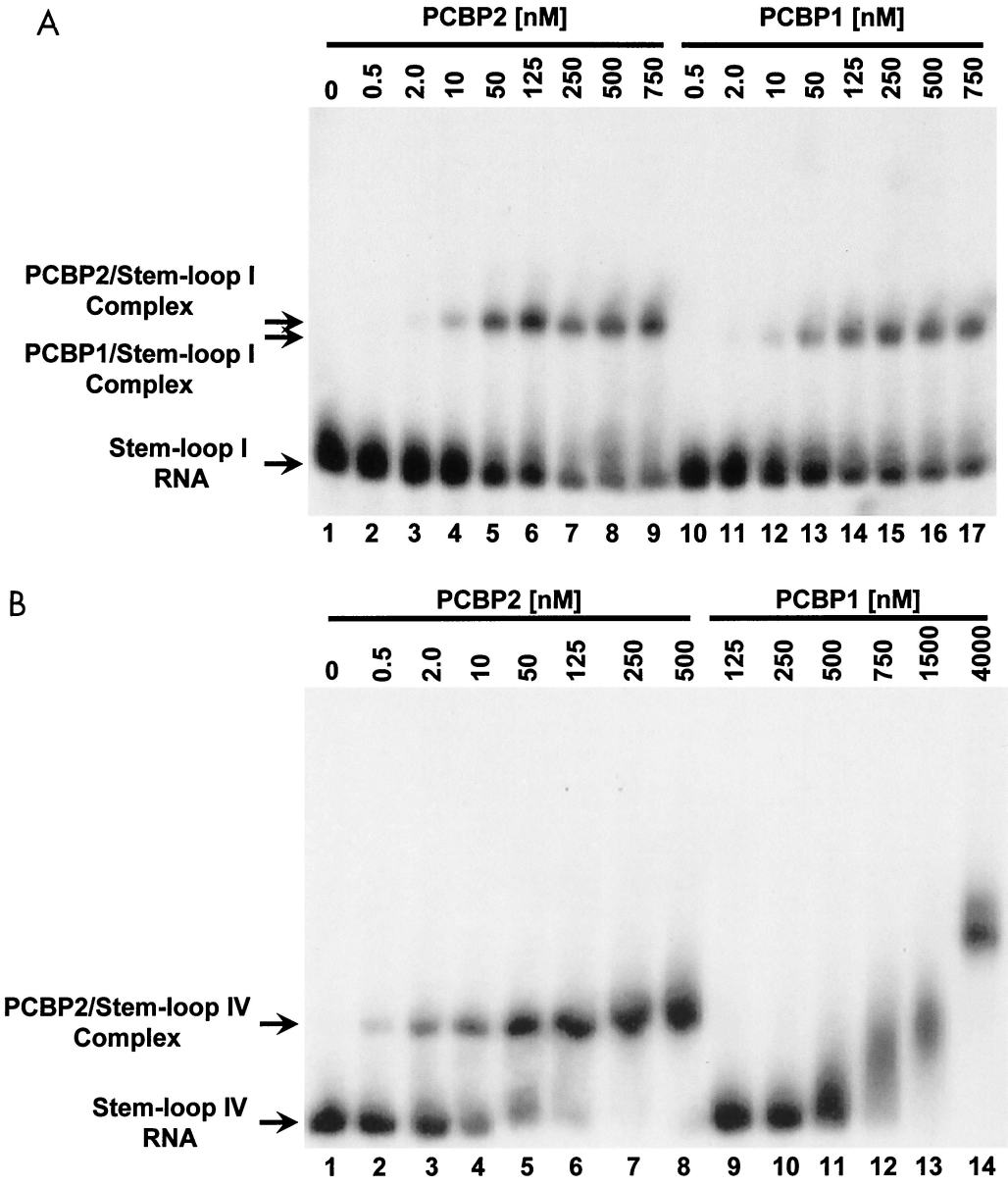

FIG. 2. RNA electrophoretic mobility shift analysis of PCBP2 and PCBP1 using stem-loop I or stem-loop IV sequences. Reaction mixtures contained a final RNA probe concentration of 0.1 nM and RNP complexes were resolved on native 4% polyacrylamide–5% glycerol–0.5× TBE gels at 4°C. (A) [α-^{32}P]UTP-labeled stem-loop I RNA was incubated with increasing molar amounts of PCBP2 (lanes 2 to 9) or PCBP1 (lanes 10 to 17). (B) [α-^{32}P]UTP-labeled stem-loop IV RNA was incubated with increasing molar amounts of PCBP2 (lanes 2 to 8) or PCBP1 (lanes 9 to 14). Lane 1 of both panels represents RNA probe incubated in buffer alone. The mobilities of the free probe and the RNP complexes are indicated. (C) Three micrograms of both the rPCBP1 (lane 1) and rPCBP2 (lane 2) protein fractions used in these and the following experiments were analyzed by electrophoresis on 12.5% polyacrylamide gels containing SDS and visualized by Coomassie blue staining. For molecular mass comparisons, the molecular masses (in kilodaltons) and relative mobilities of a set of protein standards are indicated to the right of the panel.

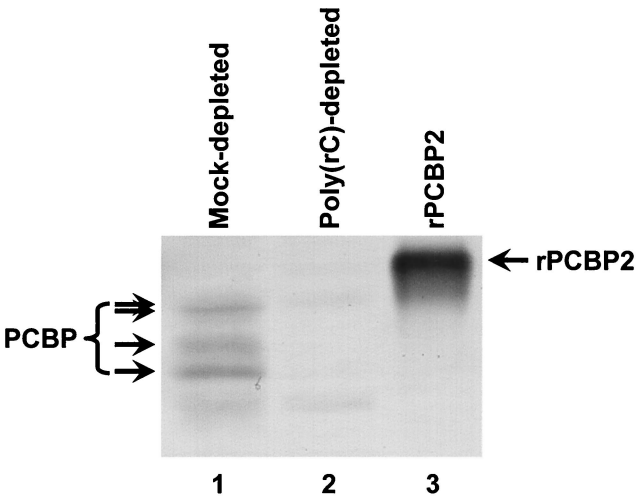

FIG. 3. Depletion of endogenous PCBP from HeLa S10 extracts by poly(rC) affinity chromatography. Forty micrograms of total protein from a mock-depleted (lane 1) or poly(rC)-depleted (lane 2) translation-replication extract was subjected to SDS-PAGE. For comparison, 250 ng of recombinant histidine-tagged PCBP2 was loaded in lane 3. Three distinct endogenous PCBP species possibly representing differentially posttranslationally modified forms of PCBP1 and PCBP2 (or other related isoforms) were resolved and detected with the α-PCBP2 polyclonal antiserum. The slowest-migrating species can be resolved as a doublet (data not shown), as indicated by two arrows. RNA affinity chromatography was carried out as described in Materials and Methods. Western blot analysis was carried out as described elsewhere (6). The source of primary antibodies was a polyclonal α-PCBP2 antiserum, and the secondary antibody was alkaline phosphatase-conjugated goat anti-rabbit (Sigma). Nitroblue tetrazolium–5-bromo-4-chloro-3-indolylphosphate 1-Step colorimetric detection (Pierce) was employed.

RNA replication. We utilized a dicistronic PV replicon to functionally uncouple translation from RNA replication by use of the EMCV IRES element to drive translation of the viral proteins that are necessary for RNA replication. Since the EMCV IRES element does not require PCBP to mediate cap-independent translation initiation in vitro (58), levels of the nonstructural PV proteins that are necessary for PV RNA replication were unaffected by PCBP depletion. Thus, we could examine the effects of PCBP depletion and PCBP1 add-back on RNA replication independently of the effects that the depletion exerts on PV IRES-mediated translation.

The T7 RNA polymerase-based transcription construct pT7RibPVE2A(MluI), utilized to generate the chimeric dicistronic PV replicon RNA RibPVE2A(MluI) (Fig. 4), was based upon pT7-PV1-E2A (42). pT7RibPVE2A(MluI) encodes an RNA that contains the entire 5′ NCR and PV structural protein coding region, P1, that is followed by a stop codon preceding the EMCV IRES, which drives translation of the PV nonstructural protein precursors P2 and P3. The P2/P3 coding region is followed by the PV 3′ NCR and a poly(A) tail. Since efficient T7 RNA polymerase-mediated transcription initiation requires the insertion of two guanosine residues at the 5′ end of a transcript, and an authentic 5′ end is important for efficient replication of PV RNA (30), an authentic 5′ end was generated by the transcription and subsequent cleavage activity of a *cis*-acting hammerhead ribozyme (12, 52) that cleaves itself and the extra guanosine residues from the transcript. Additionally, we linearized pT7RibPVE2A(MluI) with the restriction endonuclease, *Mlu*I, so that four nonauthentic nucleotides extended from the 3′ poly(A) tract of the transcript.

We used mock-depleted or poly(rC)-depleted HeLa cytoplasmic extracts programmed with RibPVE2A(MluI) RNA to examine levels of PV IRES-mediated translation by direct labeling of P1 with [^{35}S]methionine and levels of dicistronic replicon RNA replication by labeling with [α-^{32}P]CTP. The reactions that were labeled with [^{35}S]methionine were resolved by SDS–12.5% PAGE (Fig. 5A), while the replication reactions were resolved on 1.0% agarose gels (Fig. 5B). The levels of in vitro PV IRES-mediated translation can be observed by comparing the bands corresponding to the P1 structural precursor and its proteolytically processed structural products (VP0, VP1, and VP3). Upon comparison of reactions carried out in mock-depleted and poly(rC)-depleted HeLa S10 cytoplasmic extracts (Fig. 5A, compare lane 7 to lane 6), we observed a fourfold decrease in the ability of the PCBP-depleted reaction to mediate PV IRES element-directed translation. When rPCBP1 (Fig. 5A, lanes 1 to 5) was added to the PCBP-depleted reaction mixtures at increasing concentrations, no significant effect on PV IRES-mediated translation was observed. However, when rPCBP2 (Fig. 5A, lanes 9 to 13) was added, a dose-dependent increase in the levels of P1 (Table 1) and its processed products was observed. These results correlated with the in vitro binding assays, suggesting that while PCBP2 could interact with stem-loop IV RNA to form an RNP complex that was necessary to mediate cap-independent translation initiation, PCBP1, with its lower-affinity binding for stem-loop IV RNA, was not capable of efficiently forming a functional stem-loop IV RNP complex.

Because both PCBP1 and PCBP2 are capable of interacting with stem-loop I RNA with near-equal affinities, we hypothesized that the addition of either rPCBP1 or rPCBP2 to the PCBP-depleted reactions would rescue replication of the dicistronic RibPVE2A(MluI) RNA. Assessment of the levels of [α-^{32}P]CTP-labeled RibPVE2A(MluI) RNA in mock-depleted and PCBP-depleted replication reactions (Fig. 5B, compare lane 7 and lane 6) revealed a significant decrease in RNA replication upon PCBP depletion. This decrease was not the result of a diminished level of PV nonstructural protein synthesis, as the [^{35}S]methionine-labeled translation portion of this reaction showed that the levels of 3CD remained constant in all lanes (Fig. 5A). Upon the addition of increasing concentrations of rPCBP1 (Fig. 5B, lanes 1 to 5) or rPCBP2 (Fig. 5B, lanes 9 to 13), a rescue of RNA replication was observed (Table 1). A negative control reaction that contained 2 mM guanidine hydrochloride (GuHCl), a potent inhibitor of PV negative-strand RNA synthesis (8), provided evidence that the labeled product resulted from PV RNA replication.

Differential functions for the KH domains of PCBP2 in PV translation and RNA replication. The solution structures of two KH modules, one from human vigilin and the other from the fragile X mental retardation (fmr1) protein, have been solved by nuclear magnetic resonance spectroscopy (45, 46). The tertiary structure of each of these domains consists of a βααββα structure (see Fig. 6 for PCBP KH domain amino acid and secondary structure alignment) with a three-stranded antiparallel β-sheet packed against three α-helices. At the core of

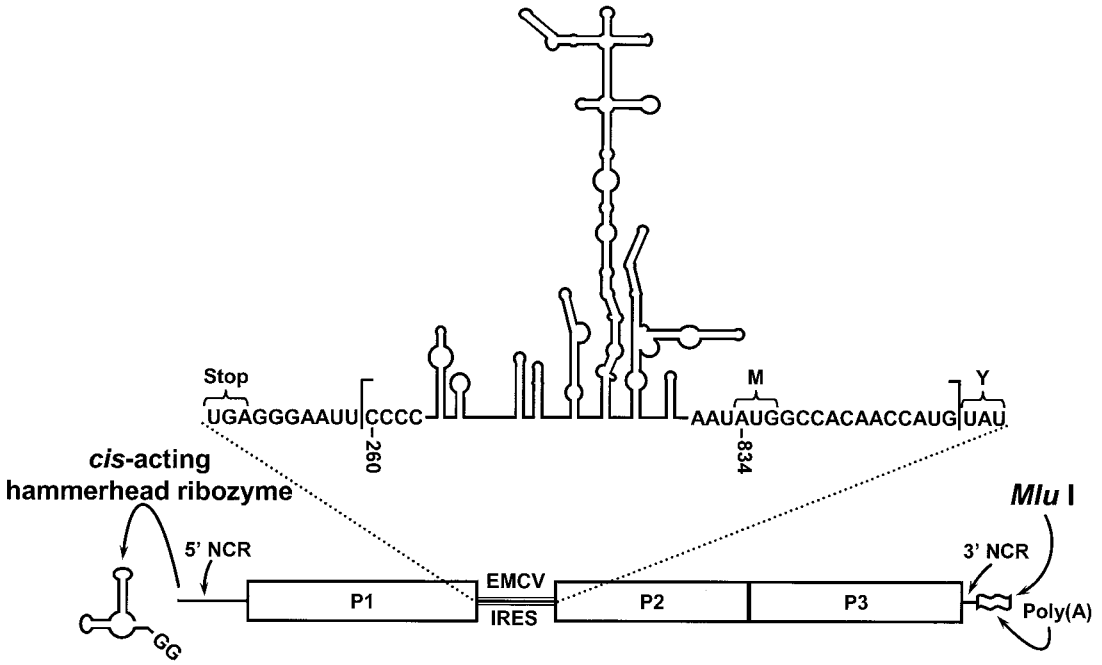

FIG. 4. Genetic organization of the dicistronic replicon RNA, RibPVE2A(MluI), transcribed from the T7 RNA polymerase-based transcription construct pT7RibPVE2A(MluI). pT7RibPVE2A(MluI) encodes an RNA that contains the entire 5′ NCR and P1 coding region of PV separated from the P2/P3 coding regions, the 3′ NCR, and a poly(A) (>30 nt in length) by the EMCV IRES element. A *cis*-acting hammerhead ribozyme enzymatically cleaves itself (and the two guanosine residues of the T7 promoter) from the RNA, leaving the transcript with an authentic 5′ end. The 3′ terminus of the transcript contains four nonviral nucleotides imparted by the *Mlu*I restriction endonuclease site utilized for template linearization. The inserted fragment (see inset) encodes a UGA stop codon (Stop) followed by a 7-nt spacer, the EMCV IRES element (EMCV nt 260 to 834) followed by the first 15 nt of the EMCV open reading frame, and an additional tyrosine codon (Y) to provide a *cis* cleavage site for the generation of an authentic P2 N terminus following cleavage by the adjacent 2A proteinase ($2A^{pro}$) activity. The initiation codon of the second cistron is indicated (M).

the KH domain is a conserved IGkxGxxI motif that is the hallmark of the KH family of RNA binding proteins. The most highly conserved portion of this motif, a GkxG tetrapeptide found between the first two α-helices (Fig. 6), is hypothesized to be an unstructured surface loop important for nucleic acid binding. The central positions of this loop are occupied by basic amino acids that are in an exposed position for interaction with negatively charged nucleic acids. Since this sequence conservation is present in a flexible loop, it cannot be explained by structural criteria and therefore must have a functional role in RNA binding (2). Other basic residues in the vicinity of the GkxG tetrapeptide have been shown to be at least in proximity to the RNA binding site, as a semiconserved negatively charged amino acid found at the C-terminal end of the second α-helix (Fig. 6) of the bacterial ribosomal protein S3 cross-links with RNA (57). Combining the above data with a noted basic residue preference and spacing conservation in the vicinity of the putative RNA-binding surface of the first and second α-helices, we hypothesized that some of these basic residues are directly involved in KH domain-RNA interactions. Furthermore, it is possible that the individual PCBP KH domains contribute differentially to the formation of PCBP/stem-loop I and PCBP/stem-loop IV RNP complexes. To examine this possibility, we targeted specific putative RNA binding residues in each of the three KH domains of PCBP2 using site-directed mutagenesis. Our mutagenesis protocol was designed to substitute nucleotides coding for the conserved basic residues found on this putative RNA binding surface to those coding for alanines. Charged amino acid-to-alanine mutagenesis is predicted to change the charged nature of solvent-exposed protein domains without causing major disruption in the overall protein conformation (11). Site-directed mutagenesis of PCBP2 sequences in pQE30-PCBP2 resulted in the plasmids pQE30-PCBP2-mKH1-2 (coding for the amino acid changes K31A, K32A, K38A, and R40A), pQE30-PCBP2-mKH2-6 (coding for the amino acid changes K121A and R124A), pQE30-PCBP2-mKH3-3 (coding for amino acid change R314A), and pQE30-PCBP2-mKH3-4 (coding for amino acid changes R305A and R314A). Figure 6 contains a depiction of the positions of the mutated residues adjacent to the wild-type (wt) PCBP1 and PCBP2 KH domain alignments. These plasmids were used for the expression and purification of recombinant mutated PCBP2 proteins that were used in separate RNA binding assays with stem-loop I (Fig. 7A) and IV (Fig. 7B) RNA probes.

The results of in vitro RNA mobility shift assays using increasing amounts of purified mutated PCBP2 proteins with 0.1 nM radiolabeled stem-loop I RNA are depicted in Fig. 7A. For comparison, the results of the same assay utilizing wt PCBP2 are depicted in Fig. 2A (lanes 2 to 9). All of the KH domain mutations severely disrupted PCBP2/stem-loop I RNP complex formation. There was no distinct complex formed with any of the mutated proteins even at the highest concentrations. The mKH1-2 protein contained the most detrimental mutations, since the free stem-loop I probe band remained rela-

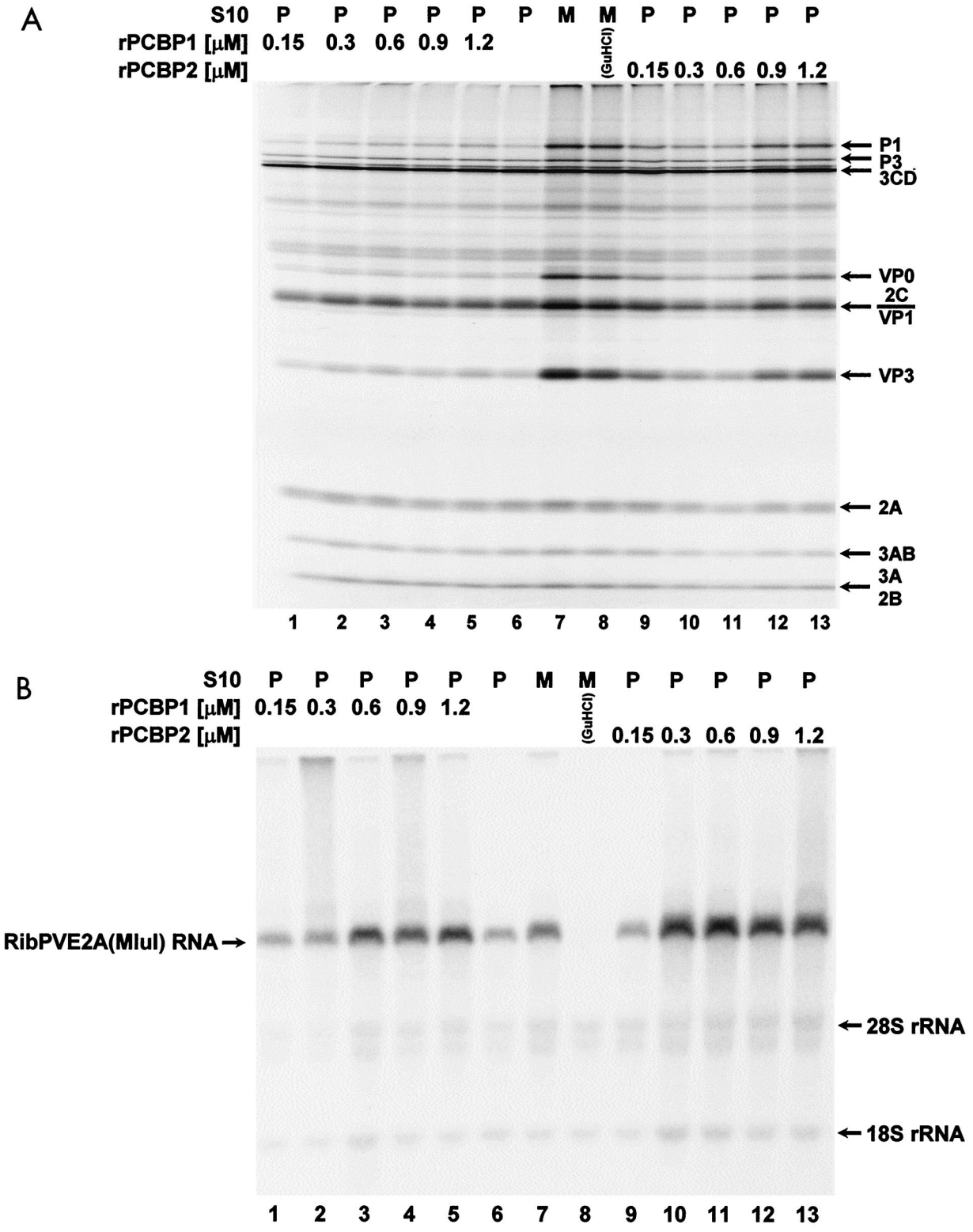

FIG. 5. Differential activities of PCBP1 and PCBP2 on PV translation and RNA replication. In vitro translation reactions and parallel in vitro RNA replication reactions carried out in either mock-depleted (M, lanes 7 and 8) or poly(rC)-depleted (P, lanes 1 to 6 and 9 to 13) HeLa S10 extracts were programmed with RibPVE2A(MluI) dicistronic replicon RNA. The reactions were supplemented to the indicated final concentration with either rPCBP1 (lanes 1-5), rPCBP2 (lanes 9 to 13), or with buffer alone (lanes 6 and 7). A negative control reaction that contained 2 mM GuHCl, a potent inhibitor of PV negative-strand RNA synthesis, was also utilized (lane 8). The phosphorimager scans depicted in both panels are the results of single experiments that have been independently replicated at least two times. (A) [^{35}S]methionine-labeled translation products were analyzed by electrophoresis on 12.5% polyacrylamide gels containing SDS. The identities of the bands representing specific PV proteins are indicated to the right of the image. (B) [α-^{32}P]CTP-labeled RNA replication products were resolved on 1.0% agarose–TBE (containing 0.1 mM EDTA) gels. The relative electrophoretic mobilities (based upon ethidium bromide staining) of in vitro-transcribed RibPVE2A(MluI) RNA, 28S rRNA, and 18S rRNA are indicated.

TABLE 1. Effects of the addition of rPCBP1 and rPCBP2 on PV RNA replication and PV IRES-mediated translation in PCBP-depleted extracts

Final concn of rPCBP (nM)	Fold stimulation over control reaction[a]			
	PCBP1		PCBP2	
	RNA replication	Translation	RNA replication	Translation
150	2.0	1.3	1.0	2.1
300	2.1	1.3	2.1	2.0
600	2.3	1.4	2.7	2.4
900	2.3	1.7	2.6	3.6
1,200	2.4	1.6	2.3	4.1

[a] Fold stimulation values represent the pixel volume of the [α-^{32}P]CTP-labeled RibPVE2A(MluI) RNA band (normalized for loading and recovery against the ethidium bromide-labeled 18S rRNA) or of the [^{35}S] methionine-labeled PV structural protein precursor (normalized for loading against the 3CD band) over the buffer control reaction pixel volume as determined by phosphorimager analysis. These data represent values obtained from the analysis of the scans presented in Fig. 5.

tively constant even in the reaction containing a 4,000 nM concentration of protein (Fig. 7A, lane 7). This result was not too surprising, as PCBP KH domain 1 has been shown to be a major contributor to PCBP RNA binding activity in both biochemical and functional assays (22, 53, 58). The remaining mutated proteins, mKH2-6, mKH3-4, and mKH3-3, although severely diminished in their ability to interact with stem-loop I RNA were able to shift some of the free probe at high concentrations of mutated protein (Fig. 7A, lanes 8 to 25).

Results of in vitro RNA mobility shift assays using increasing amounts of purified mutated PCBP2 proteins and stem-loop IV RNA are illustrated in Fig. 7B. These results demonstrated that three of the mutated proteins, mKH1-2, mKH3-4, and mKH3-3, were severely impaired in PCBP2/stem-loop IV RNP complex formation. The mKH1-2 mutation appeared to confer the most severe effect on PCBP2/stem-loop IV interactions, as dose-dependent disappearance of free probe was only observed at the highest concentrations of protein (Fig. 7B, lanes 5 to 7). Both mKH3-4 and mKH3-3 proteins were able to form diffuse RNP complexes with stem-loop IV RNA only at the highest concentrations of protein examined (Fig. 7B, lanes 17 to 19 and 21 to 23). The mutations present in the mKH2-6 protein were the least detrimental to stem-loop IV binding, as the mutated protein retained an intermediate ability to bind stem-loop IV sequences, resulting in the formation of up to three distinct RNP complexes with increasing protein concentration (Fig. 7B, lanes 8 to 13). While the precise composition of these three distinct mKH2-6/stem-loop IV complexes and the diffuse mKH3/stem-loop IV complexes is not known, our results are in agreement with similar in vitro binding studies that were previously carried out with PCBP proteins that also contained mutations in critical residues of the three KH domains (53). In these studies the conserved core motif,

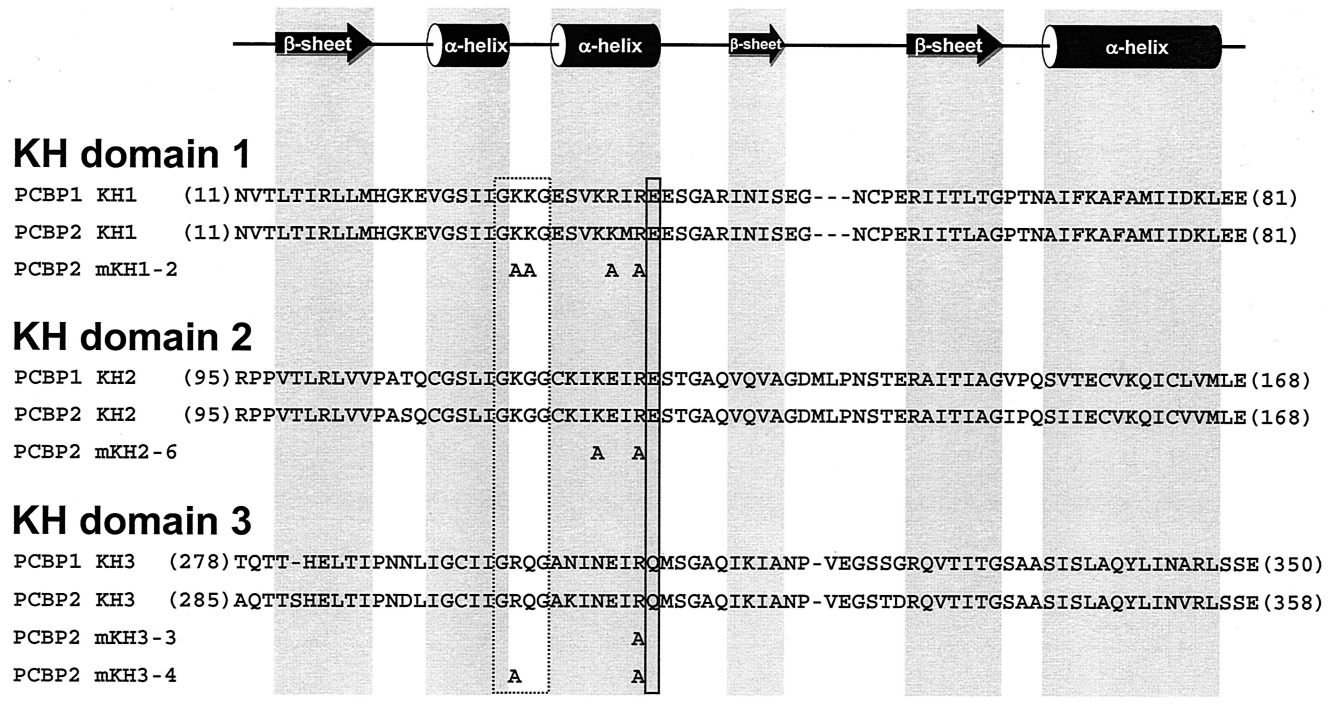

FIG. 6. Amino acid sequences and secondary structural alignments of the three KH domains of PCBP1 and PCBP2, shown adjacent to the modified residues of four mutated PCBP2 proteins. The most highly conserved tetrapeptide sequence (GkxG) contained within the KH domain is boxed (dashed box). The semiconserved residues (boxed with solid line) found at the C-terminal end of the second α-helix are homologous to a residue of the bacterial ribosomal protein S3 that cross-links with RNA. The numbers in parentheses found at the beginning and end of the amino acid sequences correspond to the residue number of the first and last residues of each domain. Secondary structural elements, α-helices (cylinders) and β-sheets (arrows), are indicated above the alignments. Structural elements and alignments were previously defined (2, 37, 41, 46). (Adapted from reference 41 with the permission of Cambridge University Press.)

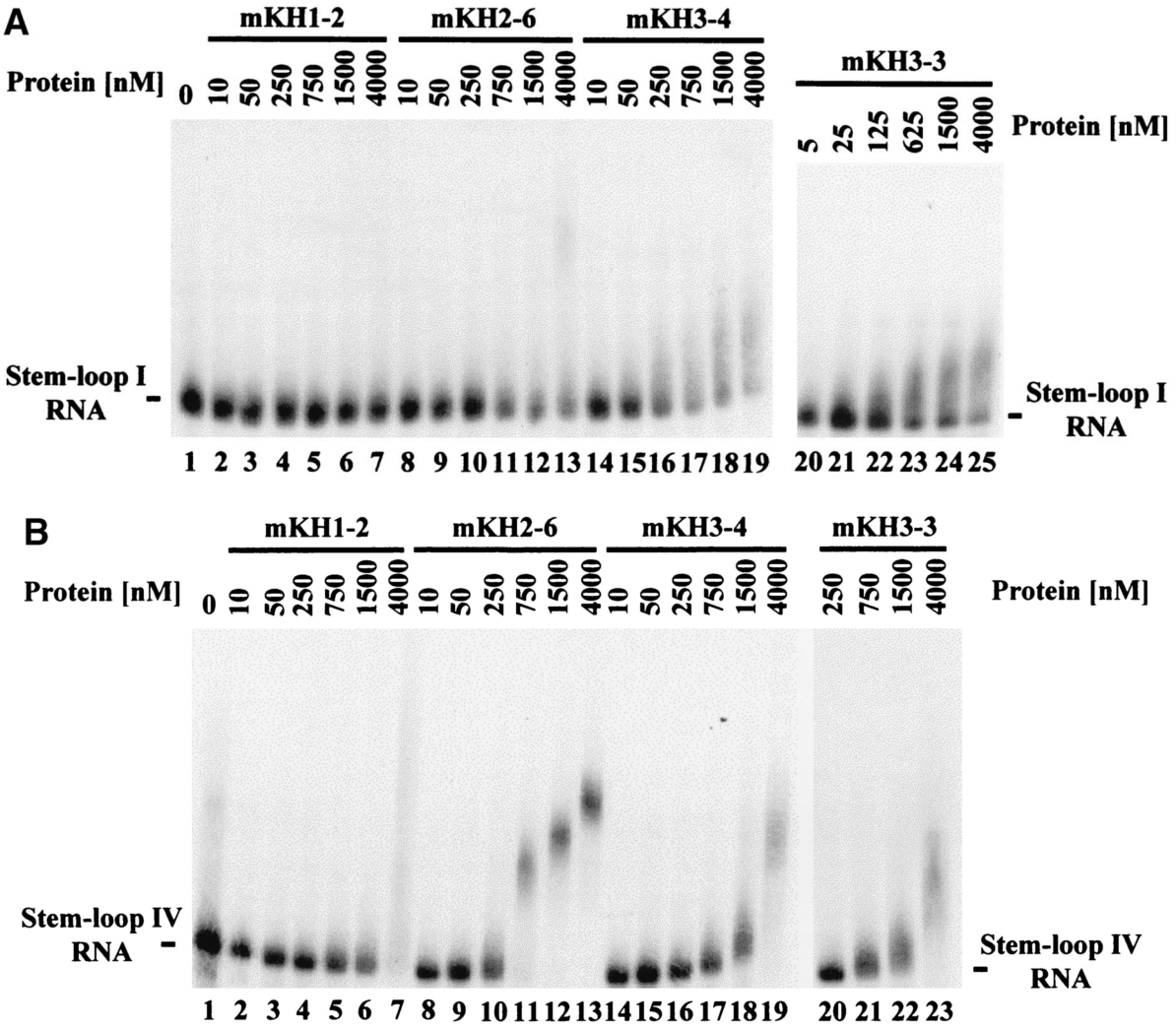

FIG. 7. RNA electrophoretic mobility shift analysis of mutated PCBP2 proteins with stem-loop I and stem-loop IV RNA sequences. Reaction mixtures contained a final RNA probe concentration of 0.1 nM and were resolved on native 4% polyacrylamide–5% glycerol–0.5× TBE gels at 4°C. (A) [α-^{32}P]UTP-labeled stem-loop I RNA was incubated with increasing molar amounts of mutated PCBP2 proteins including mKH1-2 (lanes 2 to 7), mKH2-6 (lanes 8 to 13), mKH3-4 (lanes 14 to 19), or mKH3-3 (lanes 20 to 25). (B) [α-^{32}P]UTP-labeled stem-loop IV RNA was incubated with increasing molar amounts of mutated PCBP2 proteins including mKH1-2 (lanes 2 to 7), mKH2-6 (lanes 8 to 13), mKH3-4 (lanes 14 to 19), or mKH3-3 (lanes 20 to 23). Lane 1 of both panels represents RNA probe incubated in buffer alone. The mobilities of the free probe are indicated for both panels. (C) Three micrograms of wt rPCBP2 (lane 1) and each of the mutated PCBP2 proteins, mKH1-2 (lane 2), mKH2-6 (lane 3), mKH3-3 (lane 4), and mKH3-4 (lane 5), that were used in these and the following experiments were analyzed by electrophoresis on 12.5% polyacrylamide gels containing SDS and visualized by Coomassie blue staining. For molecular mass comparisons, the molecular masses (in kilodaltons) and relative mobilities of a set of protein standards are indicated to the right of the panel.

IGkxGxxI, of each of the three KH domains was mutated to AAkxAxxI. When utilized in mobility shift analyses, the three proteins containing noncharged amino acid-to-alanine mutations revealed binding characteristics similar to those of the basic-to-alanine mutated proteins described above.

To test whether the RNA binding properties of the mutated PCBP2 proteins correlated with functions necessary for PV RNA replication and translation, we programmed the mock-depleted or poly(rC)-depleted HeLa cytoplasmic extracts with RibPVE2A(MluI) RNA. Upon comparison of the bands corresponding to the P1 structural precursor in the reactions carried out in mock-depleted and poly(rC)-depleted HeLa S10 cytoplasmic extracts (Fig. 8A, compare lane 5 to lane 4), we observed a 10-fold decrease in the ability of the PCBP-depleted reaction to mediate PV IRES element-directed translation. When increasing concentrations of mKH1-2, mKH3-3, or mKH3-4 proteins were added to the PCBP-depleted reactions, no significant effect on PV IRES-mediated translation was observed. However, when wt rPCBP2 or mKH2-6 proteins were added, a dose-dependent increase in the level of P1 and its processed products was evident (Table 2). The wt protein rescued translation to mock-depleted levels, and the mutant protein (mKH2-6) rescued translation to an intermediate level. These results correlated with the in vitro binding assay results, as wt rPCBP2 and mKH2-6 maintained high and moderate capacities to interact with stem-loop IV RNA (Fig. 2B, lanes 1 to 8, and 7B, lanes 8 to 13), respectively. Our findings reinforced the hypothesis that a high-affinity interaction of PCBP with stem-loop IV RNA is necessary for PV IRES-mediated translation. Furthermore, the mutations contained within mKH1-2, mKH3-3, and mKH3-4 diminished the affinity of these proteins for stem-loop IV RNA to levels below a threshold necessary for the efficient formation of the RNP complexes necessary for initiation of internal ribosome entry.

The levels of PV IRES-mediated translation rescued by the PCBP2 proteins with mutated KH domains correlated with the ability of these proteins to bind stem-loop IV RNA in vitro; however, the capacity of these mutated proteins to facilitate replication of the dicistronic RibPVE2A(MluI) RNA did not correlate with their abilities to interact with stem-loop I RNA in vitro. A fourfold reduction in the ability of the dicistronic RNA to replicate in the poly(rC)-depleted extracts compared to the mock-depleted extracts was observed (Fig. 8B, compare lanes 4 and 5). However, this diminished RNA replication could be rescued in a dose-dependent fashion (Fig. 8B) by the addition of mKH2-6, mKH3-3, mKH3-4, and wt PCBP2 recombinant proteins. These results were surprising in light of the fact that the ability of all of the mutated proteins to bind stem-loop I RNA was severely diminished in our in vitro binding assays (Fig. 7A). Our findings suggest that the ability to form stable RNA-protein interactions in in vitro electrophoretic mobility shift analyses may not always be a predictor of the functional nature of such interactions. On the other hand, the protein mKH1-2 contains basic-to-alanine amino acid mutations in the KH domain thought to be a primary PCBP RNA binding determinant; therefore, it was not surprising that this protein neither binds stem-loop I RNA nor rescues dicistronic RNA replication.

DISCUSSION

In this study, we have utilized in vitro RNA binding assays and in vitro PV translation-replication reactions to demonstrate that PCBP is a necessary component of two functional RNP complexes, one that forms on stem-loop IV RNA for mediation of PV IRES-driven translation and one that forms on stem-loop I RNA to mediate PV RNA replication. While one of the two major PCBP isoforms expressed in mammalian cells, PCBP2, was able to bind both stem-loop structures to mediate translation and replication, the other isoform, PCBP1, could only bind stem-loop I RNA. Thus, PCBP1 could functionally substitute for PCBP2 in the formation of an active RNA replication complex; however, PCBP1 could not efficiently bind stem-loop IV RNA to form the RNP complex that was necessary for initiation of cap-independent translation on the PV IRES element. Furthermore, our data suggest that KH domain 1 is the major RNA binding determinant contained within PCBP2. The integrity of this KH module is absolutely essential for translation initiation on the PV IRES element and for replication of PV RNA, consistent with previously published data (53). An intact second KH domain of PCBP2 is not required for the facilitation of cap-independent translation initiation on the PV IRES element or for PV RNA replication. And finally, an intact third KH module functions to mediate efficient translation initiation on the PV IRES element but is not essential for replication of PV RNA. Taken together, these data have implications for differential picornavirus template utilization during viral translation and RNA replication and suggest that specific domains of PCBP2 may have distinct roles in these activities.

Since it has been demonstrated that the RNA elongation activity of the PV 3D polymerase is not active on an RNA that is simultaneously serving as a template for translation (25) and that the presence of translating ribosomes on PV RNAs inhibits its negative-strand synthesis on these RNAs (9), it is interesting to speculate on how genomic RNA templates are selected for translation and separate templates are selected for RNA replication. During the course of the infection, when an appropriate quantity of viral proteins has been synthesized, it would be advantageous for the virus to begin to utilize the genomic RNA for synthesis of negative-strand intermediates. Given that PV has evolved to utilize a single cellular RNA binding protein, PCBP2, in both translation and RNA replication functions, it is possible that this template selection is mediated through PCBP, as originally proposed by Gamarnik and Andino (25, 26). In this model, these authors proposed that the relative abundance of the viral proteinase and polymerase precursor, 3CD, provides a gauge on the level of genomic RNA translation that has occurred. Once a sufficient level of 3CD has been translated, its interaction with stem-loop I increases the affinity of PCBP2 for stem-loop I to a level that exceeds that for stem-loop IV. In this case, the increased affinity of PCBP2 for stem-loop I results in sequestration of PCBP2 away from stem-loop IV and, therefore, inhibition of translation initiation. However, as pointed out by the authors of that paper, even at the highest concentrations of 3CD during the peak of a PV infection, the cytoplasmic PCBP concentration is sufficient to occupy both RNA targets.

Our data suggest an alternative mechanistic possibility for

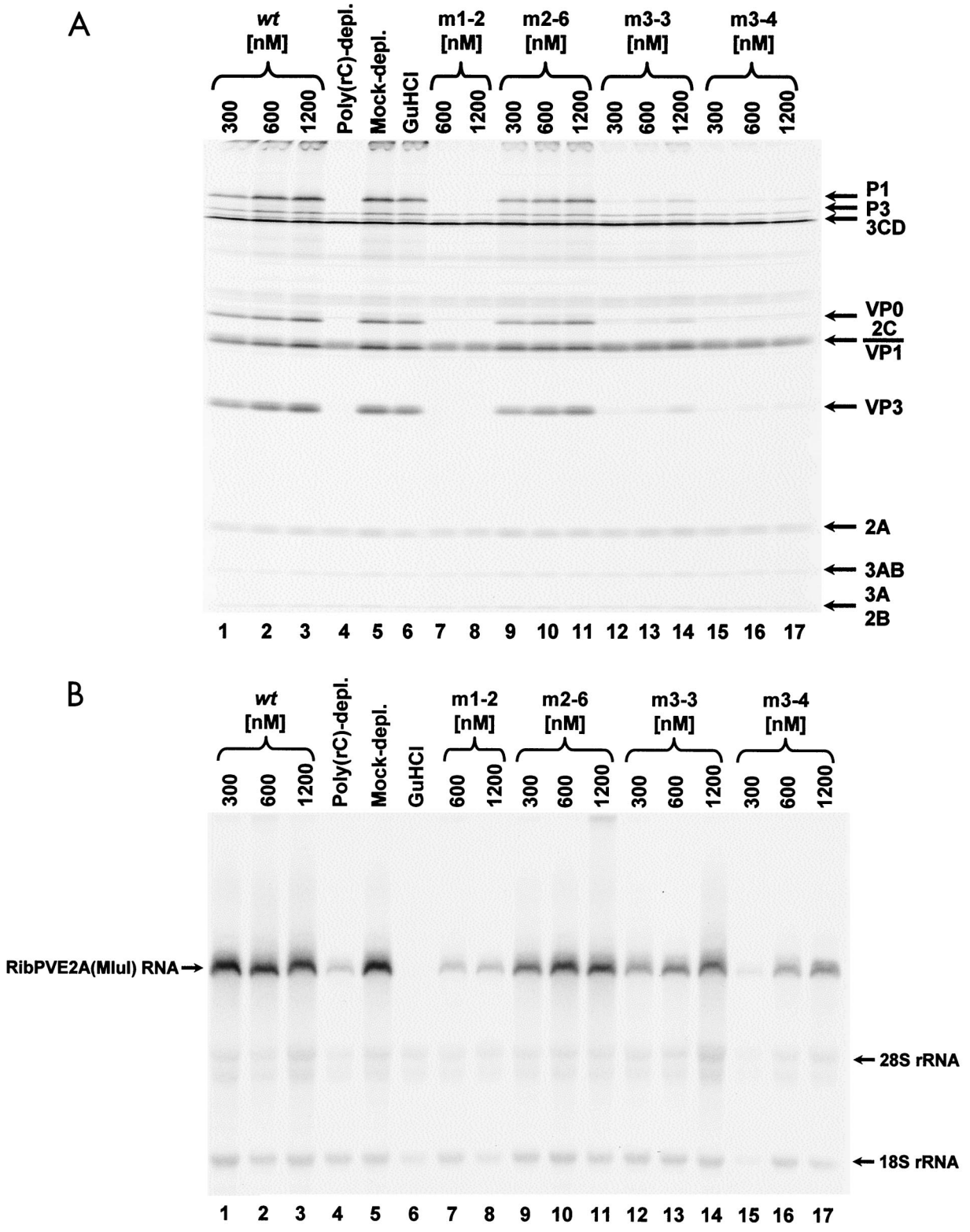

FIG. 8. Differential rescue of PV translation and RNA replication by mutated PCBP2 proteins. In vitro translation reactions and parallel in vitro RNA replication reactions carried out in either mock-depleted (lanes 5 and 6) or poly(rC)-depleted (lanes 1 to 4 and 7 to 17) HeLa S10 extracts were programmed with RibPVE2A(MluI) dicistronic replicon RNA. The reaction mixtures were supplemented at the indicated final concentrations with wt PCBP2 (lanes 1 to 3), mKH1-2 (lanes 7 and 8), mKH2-6 (lanes 9 to 11), mKH3-3 (lanes 12 to 14), mKH3-4 (lanes 15 to 17), or with buffer alone (lanes 4 and 5). A negative control reaction that contained 2 mM GuHCl was also utilized (lane 6). The phosphorimager scans depicted in both panels are the results of single experiments that have been independently replicated at least two times. (A) [^{35}S]methionine-labeled translation products were analyzed by electrophoresis on 12.5% polyacrylamide gels containing SDS. The identities of the bands representing various PV proteins are indicated to the right of the image. (B) [α-^{32}P]CTP-labeled RNA replication products were resolved on 1.0% agarose–TBE (containing 0.1 mM EDTA) gels. The relative electrophoretic mobilities (based upon ethidium bromide staining) of in vitro-transcribed RibPVE2A(MluI) RNA, 28S rRNA, and 18S rRNA are indicated.

TABLE 2. Effects of the addition of wt and mutated rPCBP2 on PV RNA replication and PV IRES-mediated translation in PCBP-depleted extracts

Final concn of rPCBP2 (nM)	Fold stimulation over control reaction[a]									
	wt PCBP2		mKH1-2		mKH2-6		mKH3-3		mKH3-4	
	Repl.	Trans.	Repl.	Trans.	Repl.	Trans.	Repl.	Trans.	Repl.	Trans.
300	3.5	8.4	ND[b]	ND	3.0	4.1	2.2	1.2	1.4	0.8
600	4.5	11.1	1.0	0.7	3.7	6.1	3.0	1.5	2.6	1.1
1,200	2.9	12.5	1.1	0.8	4.5	7.4	3.5	1.9	3.6	1.7

[a] Fold stimulation values represent the pixel volume of the [α-^{32}P]CTP-labeled RibPVE2A(MluI) RNA band (normalized for loading and recovery against the ethidium bromide-labeled 18S and 28S rRNA) or of the [^{35}S]methionine-labeled PV structural protein precursor (normalized for loading against the 3CD band) over a buffer control reaction pixel volume as determined by phosphorimager analysis. These data represent values obtained from the analysis of the scans presented in Fig. 8. Variability in the effectiveness of PCBP depletion from extract to extract resulted in the differences observed upon comparison of the fold stimulation values in Tables 1 and 2. This difference is seen when comparing the wt rPCBP2 fold stimulation values from experiments carried out in extracts that were depleted of a majority of endogenous PCBP (this table) to fold stimulation values from extracts which retained higher levels of endogenous PCBP (Table 1). Repl., replication; Trans., translation.

[b] ND, not determined.

PCBP-driven template selection during translation and RNA replication. Such a possibility assumes that PCBP2 multimerization is important for the formation of a competent translation initiation complex on the PV IRES element. This assumption is based upon observations that in vitro translation and RNA replication reactions in HeLa cell extracts partially depleted of PCBP remained competent to replicate RibPVE2A (MluI) RNA while levels of translation from the PV IRES were severely diminished (data not shown). Therefore, less PCBP2 appears to be required for PV RNA replication than is required for translation, although our RNA electrophoretic mobility shift assays (compare Fig. 2A, lanes 2 to 9, with 2B, lanes 2 to 8) demonstrated that PCBP2 has a higher affinity for stem-loop IV RNA than for stem-loop I RNA (~10- to 20-fold higher). We suggest that more PCBP2 is required for the formation of a functionally active translation complex on stem-loop IV than is required for a functional replication complex on stem-loop I because the activity of the stem-loop IV complex requires PCBP2 multimerization. Indeed, the ability of PCBP to form multimers has been previously reported (24, 34). It is possible, although speculative at this point, that the mutations contained within mKH3-3 and mKH3-4 interfere with the ability of these proteins to multimerize and form an active PCBP2/stem-loop IV RNP complex. Thus, a PV template might be selected to be a translation template if sufficient quantities of multimerized PCBP2 protein are available. However, if the quantity of PCBP2 capable of multimerization is decreased by viral protein accumulation resulting in the phosphorylation or inactivation of the PCBP2 multimerization domain or viral proteinase-mediated cleavage of PCBP2 that results in loss of the putative multimerization domain, a switch from utilization of viral template for translation to replication would occur. The validity of this model depends upon a functional role for multimerization of PCBP2 on stem-loop IV RNA, for which no experimental evidence exists. Ongoing studies to characterize the multimerization properties of wt and mutated forms of PCBP2 may resolve these possibilities.

A variation on our proposed template selection mechanism is based upon our finding that PCBP2 can mediate both PV translation initiation and RNA replication, while PCBP1 is only competent to mediate PV RNA replication. Thus, there is a pool of PCBP protein that is not capable of playing differential roles in template selection. PCBP2 and PCBP1 may be capable of forming heterodimers or hetero-multimers with differential activities in translation initiation and RNA synthesis. It is possible that a change in the relative levels of PCBP1 or PCBP2 (due to differential subcellular redistribution or proteolytic cleavage mediated by increasing concentrations of viral proteinases) could result in a change in the relative concentrations of homodimers (or homo-multimers) compared to heterodimers (or hetero-multimers), thereby altering template utilization from translation to RNA replication.

Recent data from Herold and Andino and from Flanegan and colleagues (10, 31) have led to the speculation that viral protein 3CD mediates the circularization of PV genomic RNA via its interaction with poly(A)-binding protein (PABP1) or its formation of homodimers, given that 3CD has been shown to interact with both the 5′ and 3′ NCRs of PV (4, 24, 29, 50). This proposed circularization would bring stem-loop I RNA in proximity to the appropriate template RNA for initiation of negative-strand synthesis. Additionally, Herold and Andino provided evidence that PCBP plays a role in template circularization by acting to stabilize the circular RNP complex through the reported ability of PCBP to interact with PABP1 (31, 59). A PV RNA stabilization role for PCBP was suggested by Barton and colleagues based upon their in vitro replication studies utilizing HeLa S10 extracts (44). However, their data showed a significant decrease in the stability of a PV replicon RNA without a concomitant decrease in production of negative-strand RNA.

While it is not known which combination of the above-described scenarios best illustrates the mechanism that controls the balance of viral RNAs utilized for translation versus RNA replication, it is clear that the cellular RNA binding protein PCBP is involved. Whether the PCBP/stem-loop I RNP complex is significant for the in vivo stability and/or replication of PV genomic RNA remains to be definitively determined by experiments carried out in infected cells, without the limitations imposed by this in vitro system. However, an examination of the literature suggests that while the in vitro stability of PV RNA may be dependent on PCBP, the actual in vivo role of the PCBP/stem-loop I RNP complex may be important for PV RNA replication. Furthermore, since distinct PCBP-PV RNA complexes are required for both the initiation

of translation and RNA replication, a putative role for PCBP in the selection of PV templates for translation or RNA replication is likely.

ACKNOWLEDGMENTS

We are grateful to David M. Brown for his helpful scientific discussions and critical reading of the manuscript. We also thank Raul Andino for the generous gift of prib(+)RLuc.

This work was supported by Public Health Service grant AI 26765 from the National Institutes of Health. B.L.W. was supported by a research fellowship from the American Heart Association, Western States Affiliate.

REFERENCES

1. **Aasheim, H. C., T. Loukianova, A. Deggerdal, and E. B. Smeland.** 1994. Tissue specific expression and cDNA structure of a human transcript encoding a nucleic acid binding [oligo(dC)] protein related to the pre-mRNA binding protein K. Nucleic Acids Res. **22:**959–964.
2. **Adinolfi, S., C. Bagni, M. A. Castiglione Morelli, F. Fraternali, G. Musco, and A. Pastore.** 1999. Novel RNA-binding motif: the KH module. Biopolymers **51:**153–164.
3. **Andino, R., N. Boddeker, D. Silvera, and A. V. Gamarnik.** 1999. Intracellular determinants of picornavirus replication. Trends Microbiol. **7:**76–82.
4. **Andino, R., G. E. Rieckhof, P. L. Achacoso, and D. Baltimore.** 1993. Poliovirus RNA synthesis utilizes an RNP complex formed around the 5′-end of viral RNA. EMBO J. **12:**3587–3598.
5. **Andino, R., G. E. Rieckhof, and D. Baltimore.** 1990. A functional ribonucleoprotein complex forms around the 5′ end of poliovirus RNA. Cell **63:**369–380.
6. **Ausubel, F. M., R. Brent, R. E. Kingston, D. D. Moore, J. G. Seidman, J. A. Smith, and K. Struhl.** 2000. Current protocols in molecular biology. John Wiley & Sons, New York, N.Y.
7. **Barton, D. J., and J. B. Flanegan.** 1993. Coupled translation and replication of poliovirus RNA in vitro: synthesis of functional 3D polymerase and infectious virus. J. Virol. **67:**822–831.
8. **Barton, D. J., and J. B. Flanegan.** 1997. Synchronous replication of poliovirus RNA: initiation of negative-strand RNA synthesis requires the guanidine-inhibited activity of protein 2C. J. Virol. **71:**8482–8489.
9. **Barton, D. J., B. J. Morasco, and J. B. Flanegan.** 1999. Translating ribosomes inhibit poliovirus negative-strand RNA synthesis. J. Virol. **73:**10104–10112.
10. **Barton, D. J., B. J. O'Donnell, and J. B. Flanegan.** 2001. 5′ cloverleaf in poliovirus RNA is a cis-acting replication element required for negative-strand synthesis. EMBO J. **20:**1439–1448.
11. **Bass, S. H., M. G. Mulkerrin, and J. A. Wells.** 1991. A systematic mutational analysis of hormone-binding determinants in the human growth hormone receptor. Proc. Natl. Acad. Sci. USA **88:**4498–4502.
12. **Birikh, K. R., P. A. Heaton, and F. Eckstein.** 1997. The structure, function and application of the hammerhead ribozyme. Eur. J. Biochem. **245:**1–16.
13. **Blair, W. S., J. H. Nguyen, T. B. Parsley, and B. L. Semler.** 1996. Mutations in the poliovirus 3CD proteinase S1-specificity pocket affect substrate recognition and RNA binding. Virology **218:**1–13.
14. **Blyn, L. B., R. Chen, B. L. Semler, and E. Ehrenfeld.** 1995. Host cell proteins binding to domain IV of the 5′ noncoding region of poliovirus RNA. J. Virol. **69:**4381–4389.
15. **Blyn, L. B., K. M. Swiderek, O. Richards, D. C. Stahl, B. L. Semler, and E. Ehrenfeld.** 1996. Poly(rC) binding protein 2 binds to stem-loop IV of the poliovirus RNA 5′ noncoding region: identification by automated liquid chromatography-tandem mass spectrometry. Proc. Natl. Acad. Sci. USA **93:**11115–11120.
16. **Blyn, L. B., J. S. Towner, B. L. Semler, and E. Ehrenfeld.** 1997. Requirement of poly(rC) binding protein 2 for translation of poliovirus RNA. J. Virol. **71:**6243–6246.
17. **Brown, B. A., and E. Ehrenfeld.** 1979. Translation of poliovirus RNA in vitro: changes in cleavage pattern and initiation sites by ribosomal salt wash. Virology **97:**396–405.
18. **Charini, W. A., C. C. Burns, E. Ehrenfeld, and B. L. Semler.** 1991. *trans* rescue of a mutant poliovirus RNA polymerase function. J. Virol. **65:**2655–2665.
19. **Chkheidze, A. N., D. L. Lyakhov, A. V. Makeyev, J. Morales, J. Kong, and S. A. Liebhaber.** 1999. Assembly of the α-globin mRNA stability complex reflects binary interaction between the pyrimidine-rich 3′ untranslated region determinant and poly(C) binding protein αCP. Mol. Cell. Biol. **19:**4572–4581.
20. **Collier, B., L. Goobar-Larsson, M. Sokolowski, and S. Schwartz.** 1998. Translational inhibition in vitro of human papillomavirus type 16 L2 mRNA mediated through interaction with heterogenous ribonucleoprotein K and poly(rC)-binding proteins 1 and 2. J. Biol. Chem. **273:**22648–22656.
21. **Czyzyk-Krzeska, M. F., and A. C. Bendixen.** 1999. Identification of the poly(C) binding protein in the complex associated with the 3′ untranslated region of erythropoietin messenger RNA. Blood **93:**2111–2120.
22. **Dejgaard, K., and H. Leffers.** 1996. Characterisation of the nucleic-acid-binding activity of KH domains. Different properties of different domains. Eur. J. Biochem. **241:**425–431.
23. **Dildine, S. L., and B. L. Semler.** 1992. Conservation of RNA-protein interactions among picornaviruses. J. Virol. **66:**4364–4376.
24. **Gamarnik, A. V., and R. Andino.** 1997. Two functional complexes formed by KH domain containing proteins with the 5′ noncoding region of poliovirus RNA. RNA **3:**882–892.
25. **Gamarnik, A. V., and R. Andino.** 1998. Switch from translation to RNA replication in a positive-stranded RNA virus. Genes Dev. **12:**2293–2304.
26. **Gamarnik, A. V., and R. Andino.** 2000. Interactions of viral protein 3CD and poly(rC) binding protein with the 5′ untranslated region of the poliovirus genome. J. Virol. **74:**2219–2226.
27. **Graff, J., J. Cha, L. B. Blyn, and E. Ehrenfeld.** 1998. Interaction of poly(rC) binding protein 2 with the 5′ noncoding region of hepatitis A virus RNA and its effects on translation. J. Virol. **72:**9668–9675.
28. **Haller, A. A., and B. L. Semler.** 1992. Linker scanning mutagenesis of the internal ribosome entry site of poliovirus RNA. J. Virol. **66:**5075–5086.
29. **Harris, K. S., W. Xiang, L. Alexander, W. S. Lane, A. V. Paul, and E. Wimmer.** 1994. Interaction of poliovirus polypeptide $3CD^{pro}$ with the 5′ and 3′ termini of the poliovirus genome. Identification of viral and cellular cofactors needed for efficient binding. J. Biol. Chem. **269:**27004–27014.
30. **Herold, J., and R. Andino.** 2000. Poliovirus requires a precise 5′ end for efficient positive-strand RNA synthesis. J. Virol. **74:**6394–6400.
31. **Herold, J., and R. Andino.** 2001. Poliovirus RNA replication requires genome circularization through a protein-protein bridge. Mol. Cell **7:**581–591.
32. **Holcik, M., and S. A. Liebhaber.** 1997. Four highly stable eukaryotic mRNAs assemble 3′ untranslated region RNA-protein complexes sharing cis and trans components. Proc. Natl. Acad. Sci. USA **94:**2410–2414.
33. **Kiledjian, M., X. Wang, and S. A. Liebhaber.** 1995. Identification of two KH domain proteins in the alpha-globin mRNP stability complex. EMBO J. **14:**4357–4364.
34. **Kim, J. H., B. Hahm, Y. K. Kim, M. Choi, and S. K. Jang.** 2000. Protein-protein interaction among hnRNPs shuttling between nucleus and cytoplasm. J. Mol. Biol. **298:**395–405.
35. **Kunkel, T. A.** 1985. Rapid and efficient site-specific mutagenesis without phenotypic selection. Proc. Natl. Acad. Sci. USA **82:**488–492.
36. **Leffers, H., K. Dejgaard, and J. E. Celis.** 1995. Characterisation of two major cellular poly(rC)-binding human proteins, each containing three K-homologous (KH) domains. Eur. J. Biochem. **230:**447–453.
37. **Lewis, H. A., H. Chen, C. Edo, R. J. Buckanovich, Y. Y. Yang, K. Musunuru, R. Zhong, R. B. Darnell, and S. K. Burley.** 1999. Crystal structures of Nova-1 and Nova-2 K-homology RNA-binding domains. Structure Fold. Des. **7:**191–203.
38. **Lindquist, J. N., S. G. Kauschke, B. Stefanovic, E. R. Burchardt, and D. A. Brenner.** 2000. Characterization of the interaction between αCP_2 and the 3′-untranslated region of collagen α1(I) mRNA. Nucleic Acids Res. **28:**4306–4316.
39. **Makeyev, A. V., A. N. Chkheidze, and S. A. Liebhaber.** 1999. A set of highly conserved RNA-binding proteins, αCP-1 and αCP-2, implicated in mRNA stabilization, are coexpressed from an intronless gene and its intron-containing paralog. J. Biol. Chem. **274:**24849–24857.
40. **Makeyev, A. V., and S. A. Liebhaber.** 2000. Identification of two novel mammalian genes establishes a subfamily of KH-domain RNA-binding proteins. Genomics **67:**301–316.
41. **Makeyev, A. V., and S. A. Liebhaber.** 2002. The poly(C)-binding proteins: a multiplicity of functions and a search for mechanisms. RNA **8:**265–278.
42. **Molla, A., S. K. Jang, A. V. Paul, Q. Reuer, and E. Wimmer.** 1992. Cardioviral internal ribosomal entry site is functional in a genetically engineered dicistronic poliovirus. Nature **356:**255–257.
43. **Molla, A., A. V. Paul, and E. Wimmer.** 1991. Cell-free, de novo synthesis of poliovirus. Science **254:**1647–1651.
44. **Murray, K. E., A. W. Roberts, and D. J. Barton.** 2001. Poly(rC) binding proteins mediate poliovirus mRNA stability. RNA **7:**1126–1141.
45. **Musco, G., A. Kharrat, G. Stier, F. Fraternali, T. J. Gibson, M. Nilges, and A. Pastore.** 1997. The solution structure of the first KH domain of FMR1, the protein responsible for the fragile X syndrome. Nat. Struct. Biol. **4:**712–716.
46. **Musco, G., G. Stier, C. Joseph, M. A. Castiglione Morelli, M. Nilges, T. J. Gibson, and A. Pastore.** 1996. Three-dimensional structure and stability of the KH domain: molecular insights into the fragile X syndrome. Cell **85:**237–245.
47. **Nelson, M., and M. McClelland.** 1992. Use of DNA methyltransferase/endonuclease enzyme combinations for megabase mapping of chromosomes. Methods Enzymol. **216:**279–303.
48. **Ostareck, D. H., A. Ostareck-Lederer, I. N. Shatsky, and M. W. Hentze.** 2001. Lipoxygenase mRNA silencing in erythroid differentiation: the 3′UTR regulatory complex controls 60S ribosomal subunit joining. Cell **104:**281–290.
49. **Ostareck, D. H., A. Ostareck-Lederer, M. Wilm, B. J. Thiele, M. Mann, and M. W. Hentze.** 1997. mRNA silencing in erythroid differentiation: hnRNP K

and hnRNP E1 regulate 15-lipoxygenase translation from the 3′ end. Cell **89:**597–606.
50. **Parsley, T. B., J. S. Towner, L. B. Blyn, E. Ehrenfeld, and B. L. Semler.** 1997. Poly(rC) binding protein 2 forms a ternary complex with the 5′-terminal sequences of poliovirus RNA and the viral 3CD proteinase. RNA **3:**1124–1134.
51. **Paulding, W. R., and M. F. Czyzyk-Krzeska.** 1999. Regulation of tyrosine hydroxylase mRNA stability by protein-binding, pyrimidine-rich sequence in the 3′-untranslated region. J. Biol. Chem. **274:**2532–2538.
52. **Scott, W. G.** 1997. Crystallographic analyses of chemically synthesized modified hammerhead RNA sequences as a general approach toward understanding ribozyme structure and function. Methods Mol. Biol. **74:**387–391.
53. **Silvera, D., A. V. Gamarnik, and R. Andino.** 1999. The N-terminal K homology domain of the poly(rC)-binding protein is a major determinant for binding to the poliovirus 5′-untranslated region and acts as an inhibitor of viral translation. J. Biol. Chem. **274:**38163–38170.
54. **Stefanovic, B., C. Hellerbrand, M. Holcik, M. Breindl, S. Liebhaber, and D. A. Brenner.** 1997. Posttranscriptional regulation of collagen α1(I) mRNA in hepatic stellate cells. Mol. Cell. Biol. **17:**5201–5209.
55. **Stewart, S. R., and B. L. Semler.** 1997. RNA determinants of picornavirus cap-independent translation initiation. Semin. Virol. **8:**242–255.
56. **Todd, S., J. S. Towner, and B. L. Semler.** 1997. Translation and replication properties of the human rhinovirus genome in vivo and in vitro. Virology **229:**90–97.
57. **Urlaub, H., V. Kruft, O. Bischof, E. C. Muller, and B. Wittmann-Liebold.** 1995. Protein-rRNA binding features and their structural and functional implications in ribosomes as determined by cross-linking studies. EMBO J. **14:**4578–4588.
58. **Walter, B. L., J. H. Nguyen, E. Ehrenfeld, and B. L. Semler.** 1999. Differential utilization of poly(rC) binding protein 2 in translation directed by picornavirus IRES elements. RNA **5:**1570–1585.
59. **Wang, Z., N. Day, P. Trifillis, and M. Kiledjian.** 1999. An mRNA stability complex functions with poly(A)-binding protein to stabilize mRNA in vitro. Mol. Cell. Biol. **19:**4552–4560.
60. **Weiss, I. M., and S. A. Liebhaber.** 1994. Erythroid cell-specific determinants of alpha-globin mRNA stability. Mol. Cell. Biol. **14:**8123–8132.
61. **Weiss, I. M., and S. A. Liebhaber.** 1995. Erythroid cell-specific mRNA stability elements in the α2-globin 3′ nontranslated region. Mol. Cell. Biol. **15:**2457–2465.
62. **Wimmer, E., C. U. Hellen, and X. Cao.** 1993. Genetics of poliovirus. Annu. Rev. Genet. **27:**353–436.
63. **Yu, J., and J. E. Russell.** 2001. Structural and functional analysis of an mRNP complex that mediates the high stability of human β-globin mRNA. Mol. Cell. Biol. **21:**5879–5888.